Available online at www.sciencedirect.com
SCIENCE DIRECT
Polymer 47 (2006) 2670–2676
polymer
www.elsevier.com/locate/polymer

Synthesis and characterizations of a polyimide containing a triphenylamine derivative as an interlayer in polymer light-emitting diode

Myung-Sup Jung *, Tae-Woo Lee *, Jingyu Hyeon-Lee, Byung Hee Sohn, In-Sun Jung

Materials Center, Samsung Advanced Institute of Technology, Nongseo-dong, Giheung-gu, Yongin-si, Gyeonggi-do 446-712, South Korea

Received 11 January 2006; received in revised form 8 February 2006; accepted 13 February 2006
Available online 2 March 2006

Abstract

Polyimide containing triphenylamine derivative (TPD-PI) was synthesized to prepare a polymer interlayer having insolubility in common nonpolar solvent for light-emitting polymers. *N,N′*-diphenyl-*N,N′*-bis(4-aminophenyl)-1,1-biphenyl-4,4′-diamine, as a new triphenylamine-containing diamine monomer, was synthesized by the palladium-catalyzed amination reaction between 4-nitrodiphenylamine and 4,4′-dibromobiphenyl and subsequent reduction of the nitro-intermediate. The TPD-PI was prepared from the synthesized diamine monomer and 4,4′-(hexafluoropropylidene)-diphthalic anhydride by the standard two-step polymerization method, which involved ring-opening polymerization and subsequent cyclodehydration. The structures and properties of the monomer and the resulting polyimide were characterized with ^{1}H and ^{13}C NMR, elemental analysis, gel permeation chromatography, UV–visible spectroscopy, etc. The TPD-PI is readily soluble in aprotic polar solvents such as *N*-methyl-2-pyrrolidinone and *N,N*-dimethylformamide and insoluble in nonpolar solvents such as toluene and xylene. The highest occupied molecular orbital (HOMO) level of the TPD-PI was measured to be 5.5 eV by a photoelectron spectrometer in air, and the band gap was calculated as 3.1 eV from the onset of UV–vis spectrum. The polymer light-emitting diode with the thin TPD-PI layer between a hole injection layer and an emitting polymer layer was fabricated to examine the performance of the polyimide as an polymer interlayer. Although the luminous efficiency of the device is lowered by the introduction of the TPD-PI interlayer, the lifetime of the device is improved.
© 2006 Elsevier Ltd. All rights reserved.

Keywords: Polyimide; Triphenylamine; Interlayer

1. Introduction

As the results of intensive research efforts over the past decades, great advances in the polymer light-emitting diodes (PLEDs) to apply for flat panel display have been achieved [1–4]. However, device lifetime, one of the most important factors for practical applications, still remains a serious problem for PLEDs. Especially, the lifetime of blue PLEDs [5–7] is still much shorter than those of green and red color PLED devices [8]. Some important reasons of the low device stability are known to be a poor interface structure, unbalanced carrier injection and other impurities diffused from both electrodes to the emitting layer [9–13]. To improve the balance of carrier injection and interface structure, the inclusion of a buffer layer, such as SiO_2, SiN_3, and polyimide between the anode and the light-emitting layer has been reported [14,15]. By the inclusion of those insulating materials, the stability and electroluminescence efficiency of organic light-emitting diodes (OLEDs) were significantly enhanced.

Recently, the introduction of a thin conjugated polymer interlayer between hole injection layer, such as poly(styrenesulfonate)-doped poly(3,4-ethylene dioxythiophene) (PEDOT-PSS), and light emitting layer has been reported [16]. The thin polymer interlayer blocks the radiative exitons from direct quenching by PEDOT-PSS and thus removes a nonradiative decay channel introduced by the PEDOT-PSS. This exciton blocking property of the conjugated polymer interlayer significantly improves the efficiency and lifetime of PLEDs [16]. As a thin conjugated polymer interlayer, triphenylamine-based conjugated polymers, such as poly(9,9-dioctylfluorene-*co*-bis-*N,N′*-(4-butylphenyl)-bis-*N,N′*-phenyl-1,4-phenylenediamine) (PFB) [17] and poly(9,9′-dioctylfluorene-*co*-*N*-(4-butylphenyl)diphenylamine) (TFB) [17] can be used, since such polymers are semiconductors having a wide band gap, low ionization potential, and high hole mobility due to their triphenylamine derivatives in the polymer backbone [17,18].

* Corresponding author. Tel.: +82 31 280 8264; fax: +82 31 280 9349.
E-mail addresses: msjung22@samsung.com (M.-S. Jung), taew.lee@samsung.com (T.-W. Lee).

0032-3861/$ - see front matter © 2006 Elsevier Ltd. All rights reserved.
doi:10.1016/j.polymer.2006.02.021

However, these conjugated polymers are readily soluble in the common organic solvents, such as toluene and xylene, which are also used as solvents for light-emitting polymers. Therefore, when the light-emitting polymer was spin-coated, the underlying spin-cast polymer interlayer was partially dissolved and then washed out by the solution of light-emitting polymer, or intermixed with light-emitting polymer. The thickness control of the thin conjugated polymer interlayer is, thus, fundamentally difficult, which is a serious problem for the practical use.

To overcome the problem, we focused our efforts on synthesizing polymer interlayers, which are insoluble in common nonpolar organic solvents and readily soluble in polar organic solvents. Aromatic polyimides have been widely used in the microelectronic devices and liquid crystal displays because of their excellent thermal, electrical, and mechanical properties. In several previous studies, several kinds of triphenylamine-containing polyimides were synthesized for the use of hole injecting and transporting layers for OLEDs [19–21]. These polyimides can be used as a polymer interlayer insoluble in common nonpolar organic solvent. In this article, we report the synthesis and characterizations of a polyimide having triphenylamine derivatives (TPD) on its backbone as a polymer interlayer in PLED. The spin-cast TPD-PI film is not soluble in the nonpolar solvent commonly used for the light-emitting polymer. The characteristics as a polymer interlayer of PLED will be also described herein.

2. Experimental

2.1. Materials

4-Nitrodiphenylamine, 4,4′-dibromobiphenyl, sodium *tert*-butoxide, tris(dibenzylideneacetone)dipalladium, hydrazine monohydrate, 5% palladium on activated carbon (Pd-C), and anhydrous *p*-xylene were obtained from Aldrich and used as received. Anhydrous *N*-methyl-2-pyrrolidinone (NMP) was obtained from ISP Technologies Inc. (Wayne, NJ) and dehydrated with 4 Å molecular sieves prior to use. 4,4′-(hexafluoropropylidene)-diphthalic anhydride (6FDA) was purchased from Daikin Co. (Japan) and used after vacuum drying at 130 °C for 5 h. Other chemicals were of the available commercial grade and used as received, unless otherwise mentioned.

2.2. Synthesis of N,N′-diphenyl-N,N′-bis(4-nitrophenyl)-1, 1-biphenyl-4,4′-diamine (DN-TPD)

4-Nitrodiphenylamine (2.81 g, 13 mmol), 4,4′-dibromobiphenyl (1.72 g, 5.5 mmol), sodium *tert*-butoxide (1.87 g, 19.5 mmol), and tris(dibenzylideneacetone)dipalladium (0.60 g, 0.6 mmol) were added to a refined *p*-xylene under a nitrogen atmosphere and stirred until a well-mixed solution. Then tri-*tert*-butyl phosphine (1 mL) was added thereto and the mixture was heated at 150 °C for 16 h. After the reaction was finished, the reaction mixture was cooled to room temperature, and chloroform (50 mL) was added. The resulting solution was filtered, and washed with deionized water in extraction funnel for several times. Then the solution was dehydrated with magnesium sulfate and filtered, and the solvent was removed from the filtrate under reduced pressure. The residue was purified by a silica gel column chromatography with the mixture of chloroform and *n*-hexane as an eluent. The purified product, DN-TPD, was 3.5 g (yield 50%).

^{1}H NMR (acetone-d_6, ppm): 8.17–8.09 (d, 4H), 7.82–7.75 (d, 4H), 7.54–7.47 (t, 4H), 7.38–7.30 (t, 6H), 7.09–6.99 (t, 4H). FT-IR (ATR method, cm^{-1}): 3028, 1581 (NO_2), 1486, 1316 (NO_2), 1292, 1158, 1109, 1003, 895, 831, 749, 692.

2.3. Synthesis of N,N′-diphenyl-N,N′-bis(4-aminophenyl)-1, 1-biphenyl-4,4′-diamine (DA-TPD)

The DN-TPD (3.5 g, 6.1 mmol) was dissolved in ethanol in a 250 mL three-necked flask. 0.1 g of Pd–C was then added and hydrazine monohydrate (3 mL) was added dropwise to the solution. After hydrazine monohydrate solution was completely added, the reaction was refluxed for 24 h. The mixture was then filtered to remove Pd–C. After cooling to 0 °C, the precipitated powder was isolated by recrystallization. It was purified by recrystallization from ethanol. The yield was 86%.

^{1}H NMR (DMSO-d_6, ppm): 7.49–7.41 (d, 4H), 7.27–7.20 (t, 4H), 6.99–6.89 (t, 10H), 6.88–6.80(d, 4H), 6.62–6.54 (d, 4H), 5.12–5.08 (s, 2H). ^{13}C NMR (DMSO-d_6, ppm): 147.6 (2C), 146.6 (2C), 146.3 (2C), 134.9 (2C), 132.3 (2C), 129.0 (4C), 128.1 (4C), 126.5 (2C), 121.6 (4C), 121.3 (4C), 114.9 (4C). FT-IR (ATR method, cm^{-1}): 3463 (N–H, amine), 3374 (N–H, amine), 3203, 3029, 1621,1606,1587, 1508, 1483, 1322, 1268, 1174, 1078,1024, 913, 848, 821, 759, 735, 723, 694. Elem. Anal. Calcd. for $C_{36}H_{30}N_4$: C, 83.37%; H, 5.83%; N, 10.80%. Found: C, 82.89%; H, 6.10%; N, 10.58%.

2.4. Polymerization of TPD-PI

The synthesis of TPD-PI is shown in Scheme 1. In a 100 mL round-bottom flask, 2.1 g (4 mmol) of DA-TPD was

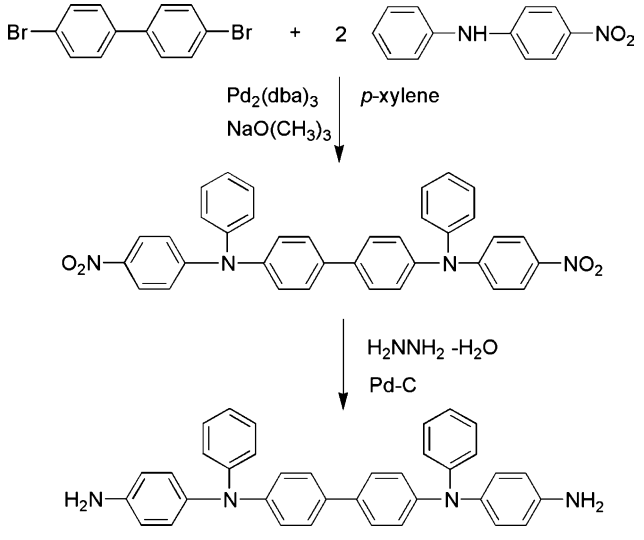

Scheme 1. Synthesis of DA-TPD.

dissolved in 20 mL of NMP. While keeping the flask at 0–5 °C, 1.8 g (4 mmol) of 6FDA was slowly added to the flask with stirring. The resulting solution was stirred at 0–5 °C for 16 h. After the polymerization, 10 mL of NMP and 10 mL of *m*-xylene was added to the flask, and the obtained poly(amic acid) was thermally imidized at 160 °C for 3 h. During this step, the water generated from its ring-closure reaction was separated as the *m*-xylene azeotrope at the same time. After the reaction was completed, the solution was slowly poured into a methanol to obtain precipitates. The precipitates were filtered and dried in a vacuum drying oven at 40 °C for 48 h.

^{1}H NMR (DMSO-d_6, ppm): 8.1–8.2 (d), 7.9–8.0 (d), 7.7(s), 7.5–7.6 (s), 7.3–7.4 (d), 7.1–7.2 (d). ^{13}C NMR (DMSO-d_6, ppm): FT-IR (ATR method, cm^{-1}): 3035, 1784 (C=O, imide), 1720 (C=O, imide), 1593, 1508, 1490, 1374 (C–N, imide), 1320, 1286, 1255,1208, 1190, 1144, 1115, 1101, 979, 963, 890, 820, 754, 721, 696, 663. Elem. Anal. Calcd for $(C_{57}H_{38}F_6N_4O_4)_n$: C, 71.54%; H, 4.00%; F, 11.91%; N, 5.85%; O, 6.69%. Found: C, 70.42%; H, 4.48%; N, 5.98%.

2.5. Measurement

^{1}H and ^{13}C NMR measurements were performed on a FT-NMR system (Bruker AVANCE 300, 300 MHz). The infrared (IR) spectrum was recorded in the range 4000–600 cm^{-1} on a FT-IR spectrometer (BIO-RAD FTS 6000) with attenuated total reflectance (ATR) method. Elemental analyses were performed with an elemental analyzer (Elementar vario EL III). The UV absorbance spectrum was obtained on a UV–visible-near-IR spectrophotometer (Shimadzu UV-3150). Gel permeation chromatography (GPC, Polymer Laboratory PL-GPC210) was performed with *N,N*-dimethylformamide (DMF)/LiBr at 40 °C at a flow rate of 1 mL/min. The weight-average and number average molecular weights were calculated with respect to polystyrene standards. Glass transition temperature (T_g) was measured with a differential scanning calorimetry (DSC, TA instruments DSC 2010) with a heating rate of 10 °C/min from 25 to 400 °C. Thermal degradation behaviors were recorded with a thermogravimetric analyzer (TGA, TA Instruments TGA 2050) at a heating rate of 10 °C/min from 50 to 700 °C in a nitrogen atmosphere. The capacitance of thin films was measured with an impedance analyzer (Hewlett–Packard 4129A). The thickness of the film was measured by using a surface profiler (Tencor P-10).

2.6. Device fabrication

For the electroluminescence (EL) studies, two devices, with and without the TPD-PI interlayer, were fabricated as follows. The indium tin oxide (ITO) glass (obtained from Samsung Corning Co.) with a sheet resistance of 10 Ω/sq was patterned in a desirable form using a photoresist and etchant, and then cleaned by successive ultrasonic treatment in a detergent, acetone and isopropyl alcohol. Then, a PEDOT-PSS solution (H.C. Starck Batron P AI4083) was spin-coated on the ITO layer to form a hole injecting buffer layer with a thickness of 50 nm and dried at 200 °C for 5 min in the glove box. The PEDOT-PSS is composed of PEDOT and PSS with a 1:6 weight ratio and the measured conductivity was 6.06×10^{-4} S/cm [22]. The TPD-PI solution (~0.8 wt% in DMF) was then spin-coated and baked at 180 °C for 1 h. Spin speed and solution concentration were regulated to obtain a 15-nm-thick film that was measured using a surface profiler. A polyspirofluorene derivative (PSF), Samsung proprietary greenish-blue-emitting polymer [23], was spin-coated with *m*-xylene solution on the TPD-PI interlayer to make a 70 nm film. It was then baked at 180 °C in vacuum for an hour to remove the solvent. Then, BaF_2, Ca, and Al with a thickness of 4, 2.7, 150 nm, respectively, were sequentially deposited on the emitting layer. The device without the interlayer was prepared in the same manner except for the spin-casting process of the TPD-PI interlayer. After encapsulating the devices in the glass cap with a UV curable resin, the current–voltage–luminescence (*I–V–L*) characteristics were obtained with a Keithley 238 source-measurement unit and a Photo Research PR650 spectrophotometer. All the measurements were performed at room temperature in air.

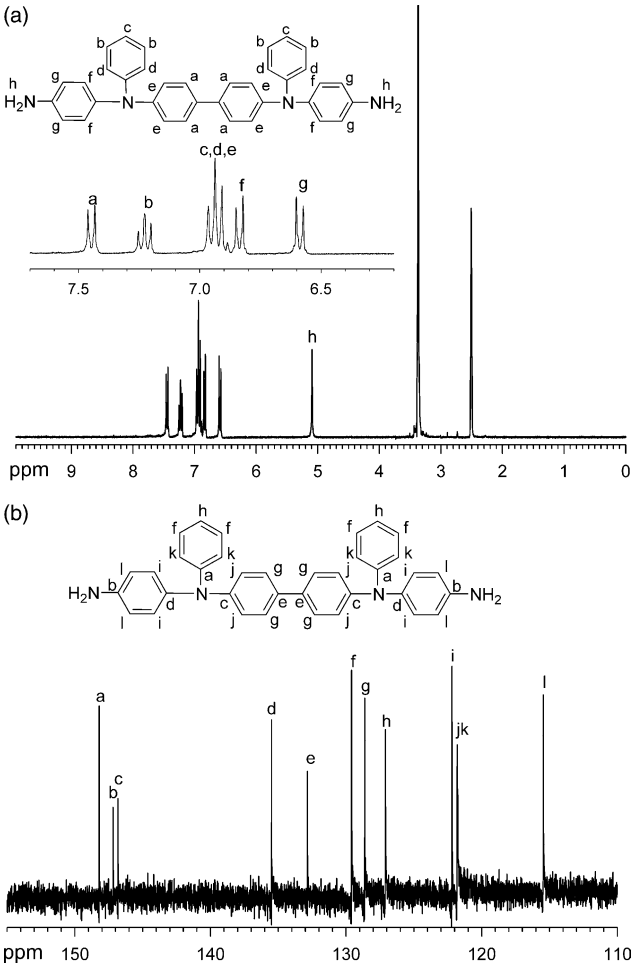

Fig. 1. ^{1}H NMR (a) ^{13}C NMR (b) spectra of DA-TPD in DMSO-d_6.

3. Results and discussion

3.1. Synthesis of monomers and polymers

The synthetic route of the new diamine monomer containing triphenylamine derivative, DA-TPD, is outlined Scheme 1. The nitro compound (DN-TPD) was synthesized by the condensation of 4-nitrodiphenylamine and 4,4′-dibromobiphenyl with the palladium-catalyzed amination [24]. FT-IR and ^{1}H NMR spectroscopic techniques were used to identify the structures of DN-TPD. In the FT-IR analysis, the nitro groups of the DN-TPD showed two characteristic bands around 1581 and 1316 cm^{-1}, which were attributed to the symmetric and asymmetric stretching of nitro groups. The catalytic hydrogenation of the dinitro compound to the diamino compound (DA-TPD) was accomplished by using hydrazine monohydrate as well as a catalytic amount of Pd–C. After the reduction, the characteristic absorptions of the nitro group disappeared and the amino group showed the typical N–H stretching absorption pair in the region of 3300–3500 cm^{-1}. The ^{1}H and ^{13}C NMR spectra also supported the formation of a desired compound having the proposed structure. As shown in Fig. 1(A) and (B), each proton and carbon was assigned to the NMR spectra of the diamine monomer.

Scheme 2 shows the schematic drawing for the polymerization of the TPD-PI. It was synthesized by the standard two-step polymerization method using DA-TPD and 6FDA, which involved ring-opening polymerization and subsequent cyclodehydration. Fig. 2 shows the IR spectrum of the TPD-PI powder. Strong band at 1780 and 1720 cm^{-1} are commonly attributed to the symmetrical and asymmetrical stretching vibrations of imide. The absorption band at 1374 cm^{-1} is due to C–N stretching and the absorptions at 1101 and 721 cm^{-1} are possibly due to imide ring deformation [25]. The ^{1}H NMR spectrum also supported the formation of a desired polymer having the proposed structure.

3.2. Basic characterization

The molecular weights were determined by GPC. The number and weight average molecular weight of the TPD-PI was found to be 12,520 and 29,360, respectively, (M_w/M_n = 2.34). The solubility behavior of TPD-PI (10 mg/mL) in different solvents was checked at room temperature. The polymer was readily soluble in aprotic polar solvents such as NMP, DMF as well as in less polar solvents such as pyridine, cyclohexanone and tetrahydrofuran.

The good solubility is due to the relatively high flexibility or free volume of macromolecular chains that are obtained by the introduction of TPD group into the structure of polyimide. Furthermore, the presence of hexafluoroisopropylidene groups of 6FDA sequences introduces a factor of asymmetry and steric hindrance that prevents a dense packing of the chains, and increases the affinity of the chains to the polar solvents [26]. The TPD-PI is completely insoluble in acetone, toluene, xylene and chlorobenzene. These results clearly show that the spin-casting process of emitting polymer in PLED fabrication does not affect the spin-cast TPD-PI interlayer.

The thermal stability of the TPD-PI was evaluated by means of TGA and DSC. As shown in TGA curve (Fig. 3), the onset temperature of weight loss is 338 °C, and the temperature of 5 wt% loss is 516.8 °C. In Fig. 4, glass transition temperature

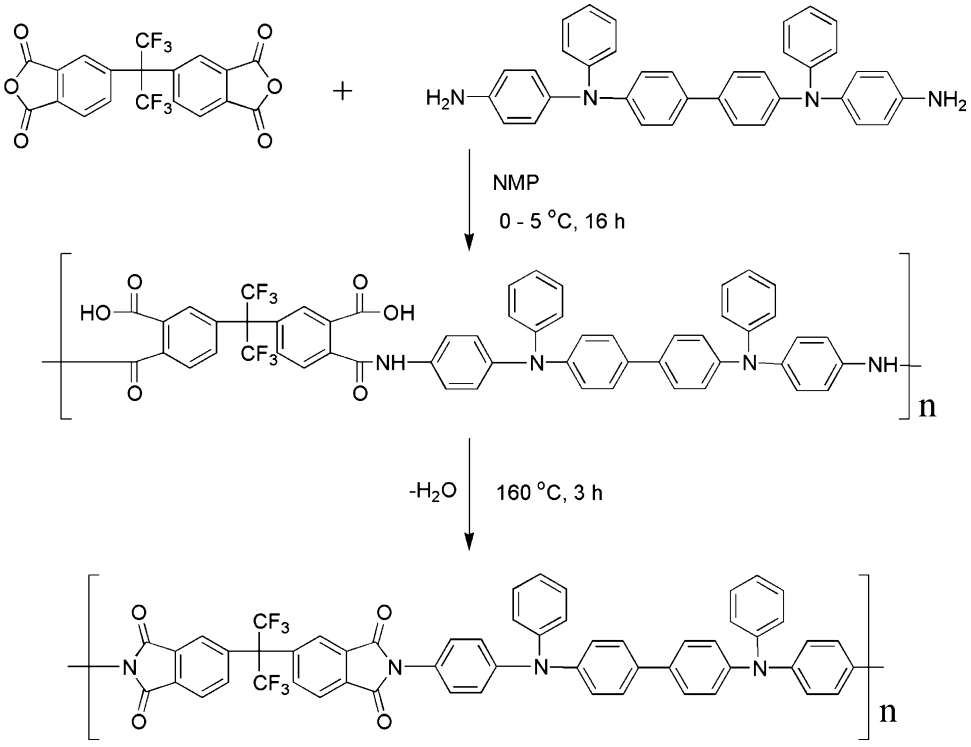

Scheme 2. Preparation of TPD-PI.

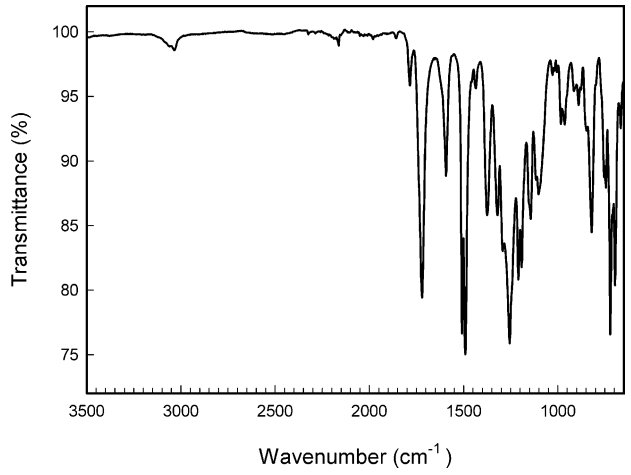

Fig. 2. FTIR spectrum of TPD-PI.

(T_g) was observed at around 306 °C by DSC. This high thermal stability of the TPD-PI could be attributed to the existence of bulky TPD moieties in the polymer backbone. In general, the chain rigidity increases due to the pendant cardo group, which restricts the free rotation of the polymer backbone [26].

3.3. Optical and photoelectron spectroscopic properties

UV–vis absorption spectrum of the TPD-PI in DMF solution was shown in Fig. 5. The maximum absorption wavelength (λ_{max}) of TPD-PI was 357 nm. The optical band gap of the TPD-PI can be calculated as approximately 3.1 eV from the onset wavelength of ca. 404 nm in the absorption spectrum.

The HOMO level of the TPD-PI is measured by a photoelectron spectrometer in air (PESA, Riken Keiki Co. AC-2, Japan). This technique gives a direct measure of the HOMO energy (ionization potentials) in air. As shown in Fig. 6, the PESA measurement of the TPD-PI indicates the HOMO level lies at −5.5 eV with respect to the vacuum level. From this PESA result and the band gap calculated from the onset of the UV–vis absorption spectrum, the lowest occupied molecular orbital (LUMO) level of the TPD-PI was estimated as ca. 2.4 eV.

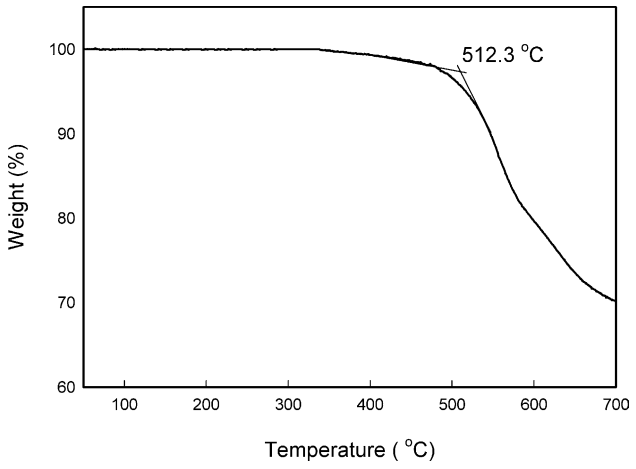

Fig. 3. TGA curve of TPD-PI.

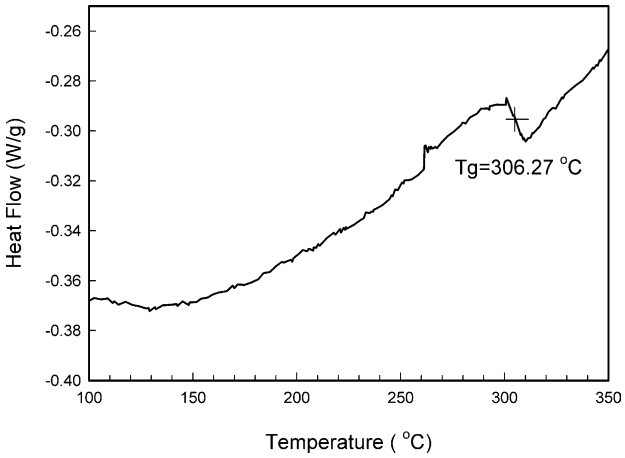

Fig. 4. DSC thermogram of TPD-PI powder.

3.4. Characteristics of PLEDs

Two PLEDs, with and without the TPD-PI interlayer, were prepared to investigate the effect of the interlayer introduced between the PEDOT-PSS and the light-emitting polymer. The PEDOT-PSS was used as a hole injection layer (HIL) to improve the device efficiency and stability because it enhances a hole injection from the ITO (work function: ∼4.7–5.0) and planarizes the ITO surface. The blue emitting polymer, PSF, was introduced with a 70 nm thickness, which has a bandgap energy of ∼2.7 eV and HOMO level of ∼5.3 eV.

The EL spectra of the devices are displayed in Fig. 7. The PLED without the interlayer emits blue light and its maximum EL peak (λ_{max}) is positioned at 480 nm. In general, when a conventional conjugated polymer such as TFB or PFB as an interlayer was introduced between the PEDOT-PSS and the emitting layer, the EL spectrum was slightly bathochromic shifted due to the increased optical cavity length between ITO and cathode. However, upon the introduction of the TPD-PI layer between the PEDOT-PSS and the emitting layer, the EL spectrum was not significantly changed. The Commission Internationale de l'Eclairage (CIE) 1931 coordinates was also slightly shifted form (0.146, 0.327) to (0.143, 0.288) by the

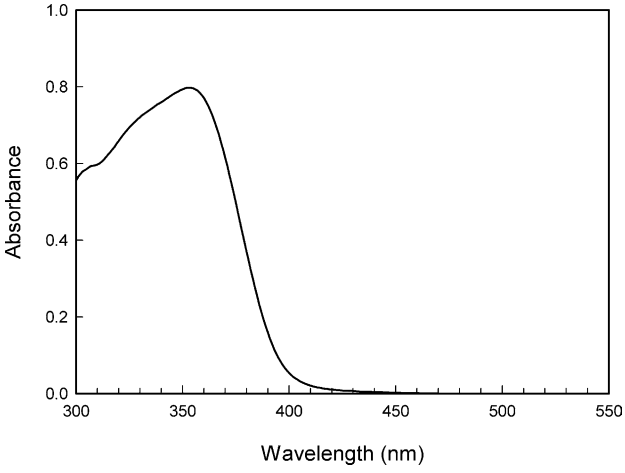

Fig. 5. UV–vis spectrum of TPD-PI.

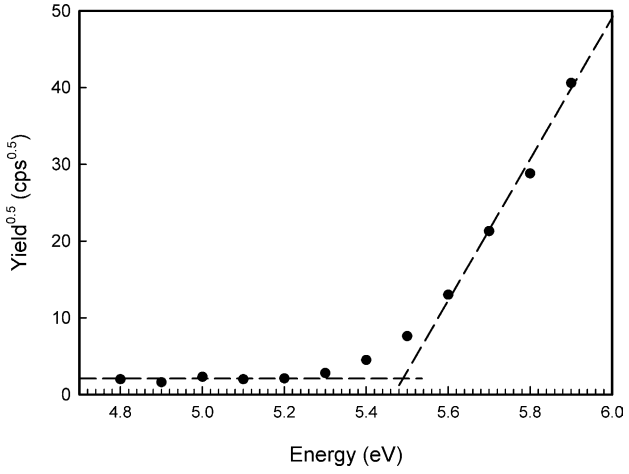

Fig. 6. Photoelectron spectrum of TPD-PI measured by PESA.

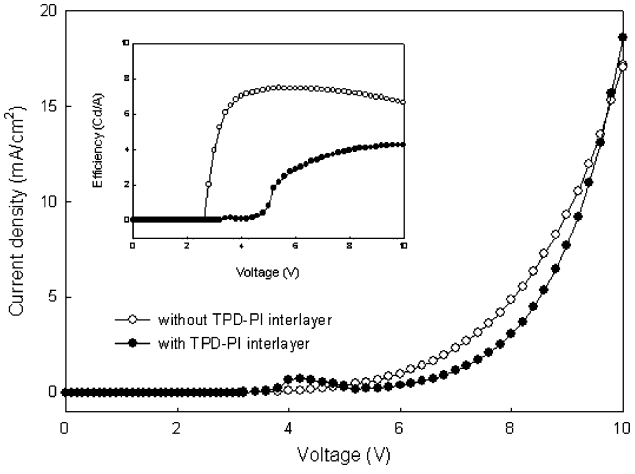

Fig. 8. *I–V* characteristics and luminous efficiencies (inset) of the devices with and without the TPD-PI interlayer.

introduction of the TPD-PI layer. We assumed that the slight change was originated from the difference of the applied voltage between two devices.

Fig. 8 shows the current–density/voltage characteristics of the devices. The current density increased with an increasing forward bias voltage, and this is a typical diode characteristic. The turn-on voltages of the PLED without and with the TPD-PI interlayer were 2.6 and 3.0 V for eye detection, respectively, and the two devices show a similar behavior in their *I–V* curves. However, the luminous efficiency was lowered to almost half of the by the introduction of the TPD interlayer (inset of Fig. 8). This means that the device with the TPD-PI interlayer is relatively less balanced than that without the interlayer. The unbalanced injection in the device with the interlayer can be explained from the band diagram shown in Fig. 9. In the case of the PLED without the TPD-PI interlayer, the interface between the PEDOT-PSS and the emitting layer is nearly ohmic contact, since there is a slight difference in energy level for hole injection from the PEDOT-PSS to the light-emitting polymer. However, when the TPD-PI interlayer is introduced in the PLED, it plays a role as an energy barrier against hole injection from the PEDOT-PSS layer to the emitting layer. The hole injection from the valence band of the PEDOT-PSS into the light-emitting polymer via the TPD-PI was more inhibited than the direct injection from the PEDOT-PSS into the light-emitting polymer due to the energy barrier between the PEDOT-PSS and the TPD-PI. The decrease in the device efficiency can be also ascribed to the low hole transporting capability of the TPD-PI backbone, which consists of insulating imide units and charge transporting TPD units. Thus, the amounts of holes injected to the emitting layer can be relatively low compared with that of the PEDOT-PSS. However, the high efficiency of a PLED device does not always lead to high stability as reported previously [27].

We also tested the lifetime of the devices with and without the TPD-PI interlayer at an initial luminance of 800 cd/m^2 after 15 min aging at 800 cd/m^2. The driving current density of the devices with and without the TPD-PI interlayer is 11.2 and 17.7 mA/cm^2, respectively. As shown in Fig. 10, in spite of the higher driving current density of the device with the TPD-PI interlayer than that of the device without the TPD-PI interlayer, the lifetime is ~1.6 times improved. Although the efficiency of the device is lowered by the introduction of the TPD-PI interlayer, the lifetime of the device is improved. This result implies that the TPD-PI interlayer acts as a buffer layer to

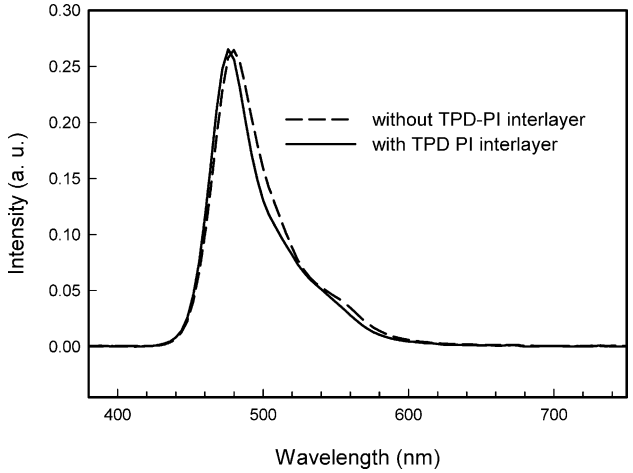

Fig. 7. EL spectra of PLEDs with and without the TPD-PI interlayer.

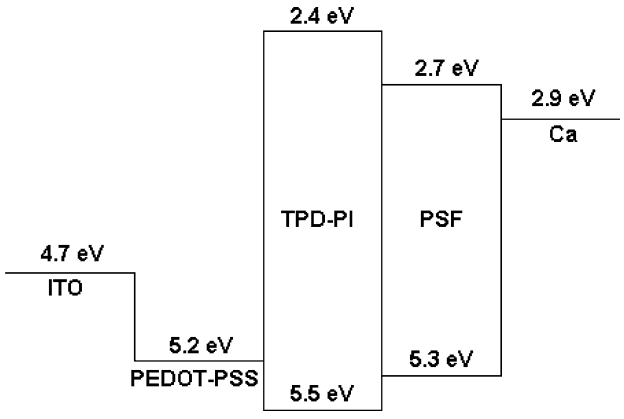

Fig. 9. Energy band diagram of the PLED composed of ITO/PEDOT-PSS//TPD-PI/PSF/Ca.

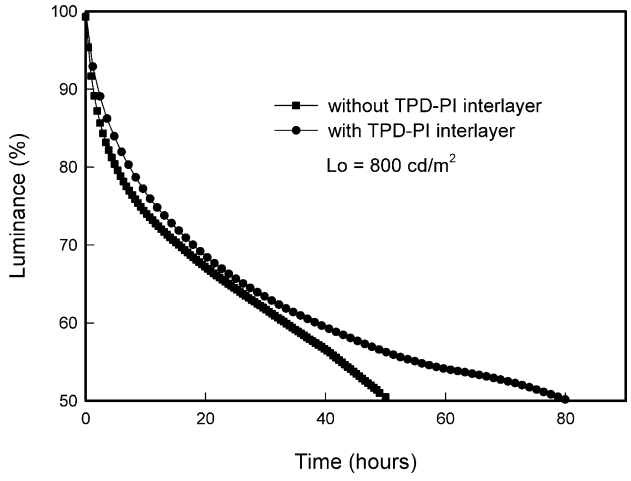

Fig. 10. The luminance decay of the devices with and without the TPD-PI interlayer as a function of time. The initial luminance was 800 cd/m^2.

prevent the adverse effects of the PEDOT-PSS layer on the emitting layer. The recent investigations on failure mode of PLEDs suggested that the PEDOT-PSS itself could be one of the dominant failure reasons owing to its residual impurities such as sodium and sulfate, and electron-induced degradation [28]. The TPD-PI interlayer may, thus, play a role in blocking the migration of the impurities, such as sodium and sulfate, from the PEDOT-PSS layer to the emitting layer and the degradation induced by injected electrons during the operation. The PEDOT-PSS (Baytron P AI4083) contains ca. 400 ppm of sodium and ca. 40 ppm of sulfate [29]. On the basis of the results, the synthesized TPD-PI shows a great potential as an polymer interlayer for the practical applications of PLEDs. We are now under investigation about the exact mechanism of the lifetime enhancement.

4. Conclusions

A novel TPD-PI was synthesized for the use of polymer interlayer in PLEDs. As a diamine monomer, DA-TPD was synthesized and polymerized with 6FDA. The TPD-PI has a high solubility in aprotic polar solvent and is completely insoluble in common nonpolar solvent for light-emitting polymers, which is a prerequisite property for the practical use as a polymer interlayer in PLEDs. Furthermore, the polyimide exhibits high thermal stability and wide band gap property due to its TPD moiety in the polymer backbone.

The luminous efficiency of the device is lowered by the introduction of TPD-PI interlayer due to the increased energy barrier between the PEDOT-PSS layer and the emitting layer, and low hole injection property of the TPD-PI. However, the lifetime of the device is ca. 1.6 times improved, which is due to the effective blocking of adverse effects by the PEDOT-PSS such as the migration of impurities from the PEDOT-PSS layer to the emitting layer. The novel polyimide, from the results, shows a great potential as a new type of polymer interlayer due to its wide band gap, insolubility in nonpolar solvent, excellent electrochemical and thermal stability.

References

[1] Burroughes JH, Bradely DDC, Brown AR, Marks RN, Mackay K, Friend RH, et al. Nature 1990;347:539.
[2] Kraft A, Grimsdale AC, Holmes AB. Angew Chem, Int Ed 1998;37:402.
[3] Cao Y, Parker ID, Yu G, Zhang C, Heeger AJ. Nature 1999;397:414.
[4] Friend RH, Gymer RW, Holmes AB, Burroughes JH, Marks RN, Taliani C, et al. Nature 1999;397:121.
[5] Scherf U, List EJW. Adv Mater 2002;12:477.
[6] Lee KS, Kim YH, Lee Y, Jang J, Kwon SK. J Polym Sci, Part A: Polym Chem 2005;43:2316.
[7] Liu SP, Chan HSO, Ng SC. J Polym Sci, Part A: Polym Chem 2005;42:4792.
[8] Jacob J, Oldridge L, Zhang J, Gaal M, List EJW, Grimsdale AC, et al. Curr Appl Phys 2004;4:339.
[9] Schlatmann AR, Floet DW, Hilberer A, Garten F, Smulders PJM, Klapwijk TM, et al. Appl Phys Lett 1996;69:1764.
[10] Jabbour GE, Shaheen SE, Kawabe Y, Morrel MM, Cho SJ, Wang JF, et al. Proc SPIE 1997;3148:2.
[11] Scott JC, Kaufman JH, Brock PJ, DiPietro R, Salem J, Goitia JA. J Appl Phys 1996;79:2745.
[12] Cumpston BH, Parker ID, Jensen KF. J Appl Phys 1997;81:3716.
[13] Kim JS, Ho PKH, Murphy CE, Baynes N, Friend RH. Adv Mater 2002;14:206.
[14] Deng ZB, Ding XM, Lee ST, Gambling WA. Appl Phys Lett 1999;74:2227.
[15] Cho SJ, Park DK, Kwon TW, Yoo DS, Kim IG. Thin Solid Films 2002;417:175–9.
[16] Kim JS, Friend RH, Grizzi I, Burroughes JH. Appl Phys Lett 2005;87:023506.
[17] Redecker M, Bradley DDC, Inbasekaran M, Wu WW, Woo EP. Adv Mater 1999;11:241.
[18] Kim JS, Ho PKH, Murphy CE, Friend RH. Macromolecules 2004;37:2861.
[19] (a) Cheng SH, Hsiao SH, Su TH, Liou GS. Polymer 2005;46:5939.
(b) Cheng SH, Hsiao SH, Su TH, Liou GS. Macromolecules 2005;38:307.
[20] (a) Imai Y, Ishida M, Kakimoto MA. High Perform Polym 2003;15:281.
(b) Liaw DJ, Hsu PN, Chen WH, Lin SL. Macromolecules 2002;35:4669.
[21] Kim Y, Han K, Ha CS. Macromolecules 2002;35:8759.
[22] The material information is available in the H.C. Starck website. http://www.hcstrack.com.
[23] Son JM, Park SH, Lee JH, Baek WJ, Sato H. US Patent 2004-0072989 A1.
[24] Yamamoto T, Nishiyama M, Koie Y. Tetrahedron Lett 1998;93:2367.
[25] Cheng SH, Hsiao SH, Su TH, Liou GS. Macromolecules 2005;38:307.
[26] Xu S, Yang M, Wang J, Ye H, Liu X. Synth Met 2003;32:145.
[27] Kim J, Lee J, Han CW, Lee NY, Chung IJ. Appl Phys Lett 2003;82:4238.
[28] Crispin X, Marciniak S, Osikowicz W, Zotti G, Gon AWDVD, Louwet F, et al. J Polym Sci, Part A: Polym Chem 2003;41:2561.
[29] The information was supplied by H.C. Starck. http://www.hcstarck.com.